Springer

KSME

Journal of Mechanical Science and Technology 28 (1) (2014) 245~253
www.springerlink.com/content/1738-494x
DOI 10.1007/s12206-013-0962-5

Numerical methodologies for investigation of moderate-velocity flow using a hybrid computational fluid dynamics – molecular dynamics simulation approach †

Soon-Heum Ko[1], Nayong Kim[2,*], Shantenu Jha[3], Dimitris E. Nikitopoulos[4] and Dorel Moldovan[4]

[1]*National Supercomputing Centre, Linköping University, Linköping, 584 32, Sweden*
[2]*Center for Computation and Technology, Louisiana State University, Baton Rouge, LA, 70803, USA*
[3]*Department of Electrical and Computer Engineering, Rutgers University, Piscataway, NJ, 08854, USA*
[4]*Department of Mechanical and Industrial Engineering, Louisiana State University, Baton Rouge, LA, 70803, USA*

(Manuscript Received July 23, 2012; Revised May 26, 2013; Accepted July 30, 2013)

Abstract

Numerical approaches are presented to minimize the statistical errors inherently present due to finite sampling and the presence of thermal fluctuations in the molecular region of a hybrid computational fluid dynamics (CFD) - molecular dynamics (MD) flow solution. Near the fluid-solid interface the hybrid CFD-MD simulation approach provides a more accurate solution, especially in the presence of significant molecular-level phenomena, than the traditional continuum-based simulation techniques. It also involves less computational cost than the pure particle-based MD. Despite these advantages the hybrid CFD-MD methodology has been applied mostly in flow studies at high velocities, mainly because of the higher statistical errors associated with low velocities. As an alternative to the costly increase of the size of the MD region to decrease statistical errors, we investigate a few numerical approaches that reduce sampling noise of the solution at moderate-velocities. These methods are based on sampling of multiple simulation replicas and linear regression of multiple spatial/temporal samples. We discuss the advantages and disadvantages of each technique in the perspective of solution accuracy and computational cost.

Keywords: Hybrid CFD-MD approach; Nanofluidics; Replica sampling; Spatial regression; Molecular statistical errors (molecular sampling noise); Temporal regression

1. Introduction

The hybrid computational fluid dynamics/molecular dynamics (CFD-MD) simulation methodology [1-9] is a reliable simulation approach capable of accurately describing the flow characteristics at mesoscales (in the 10 nm – 1 μm range). Many open-source CFD solvers of today [10-13] provide efficient and accurate flow solutions in the continuum regime. While this approach is very successful at modeling behavior of fluids from laminar flow, to turbulent flow, to high Mach number gas dynamics, it inherently lacks the capability to accurately capture complex physical and chemical interactions at fluid-fluid and fluid-solid interfaces. It is at the interface where molecular dynamics (MD) simulation can provide a more accurate atomistic description of these phenomena [14-16]. However, MD simulations have limitations when used to simulate realistic physical conditions, mostly due to the disparate spatial and temporal scales that have to be resolved in such simulations. Hybrid CFD-MD methodologies based on combination of the continuum and MD approaches have the capabilities to take advantage of both the efficiency of CFD models and the accuracy at the interfaces of MD models. In a hybrid CFD-MD approach, the continuum hypothesis is adopted in capturing macroscopic flow features, and a particle-based technique captures the intermolecular interactions near interfaces. These continuum and molecular domains are coupled through an overlap region that facilitates the exchange of information between them and satisfies the physics of the process at both levels (see Ref. [2] for example). The two descriptions are constrained to match each other by constrained molecular dynamics and boundary conditions based on time and spatial averaging of relevant physical properties in the overlap region. In this manner, the hybrid approach provides a good balance between computational cost and atomistic details/resolution where it is needed.

Despite some clear advantages over standard CFD or MD methodologies, the application of hybrid CFD-MD simulation techniques so far has been limited. In many of the previous applications in order to prevent the sampling noise of molecular properties from decreasing the accuracy of a solution, the flow conditions used were rather artificial, characterized in

*Corresponding author. Tel.: +1 225 578 5486, Fax.: +1 225 578 5362
E-mail address: nykim@cct.lsu.edu
† Recommended by Associate Editor Dae Joong Kim

general by relatively high flow velocities. It is established that any sampling over finite spatial/temporal scales induces noise, which can be diminished by increasing sampling scales. While one can reduce the noise due to spatial averaging by increasing the size of the MD region, the methodologies for controlling the noise level due to temporal averaging are more complex and more sensitive to simulation parameters. Therefore, there is a need for a systematic development of numerical approaches that would improve the capabilities of hybrid CFD-MD simulation methodologies in simulating flow at moderate and low-velocities.

We introduce numerical approaches that can be used to decrease the sampling noise within an acceptable increase computational cost. The hybrid simulation technique used here and its formulation is introduced in Sec. 2. The characteristics of the statistical errors in hybrid CFD-MD simulations are introduced in Sec. 3, along with novel numerical approaches to control the noise level, such as multiple replica sampling, linear regression of multiple consecutive spatial/temporal samples. The efficiency of the numerical approaches for noise reduction is tested and validated in the context of the classical impulsively-started transient Couette flow problem and presented in Sec. 4. Concluding remarks are in Sec. 5.

2. Numerical modeling

2.1 Hybrid CFD-MD simulation approach

The CFD simulation approach can be used to accurately predict flow properties in conventional moderate/large sized fluid domains, but it has intrinsic limitations in describing the flow at the fluid-solid interface region when molecular level effects are important. While the standard classical MD simulation uses atomistic level resolution to describe interactions between atoms and molecules, and therefore provides reliable description of the flow in the interface region, it is computationally demanding when the size of the simulated system increases and impractical for simulating large systems. Therefore, neither method is suitable for resolving multi-scale flows in large systems where both molecular-level interfacial and bulk flow characteristics are important. The compromise would be to use a hybrid CFD - MD methodology, which is a reliable simulation approach capable of taking advantage of both the efficiency of CFD models and the accurate physical representation at the interfaces of MD models.

In the hybrid CFD-MD approach the system is divided into two regions with the continuum model applied to one domain and molecular dynamics to the other (usually located close to the fluid-solid interface). The two domains are coupled through an overlap region that facilitates the exchange of information between them enforcing the consistency of the two solutions. This is done by imposing constrained dynamics on the MD formulation and boundary conditions for the CFD formulation based on time and spatial averaging of the relevant physical properties in the overlap region (see Fig. 1). In the overlap region, the computational domain is decomposed

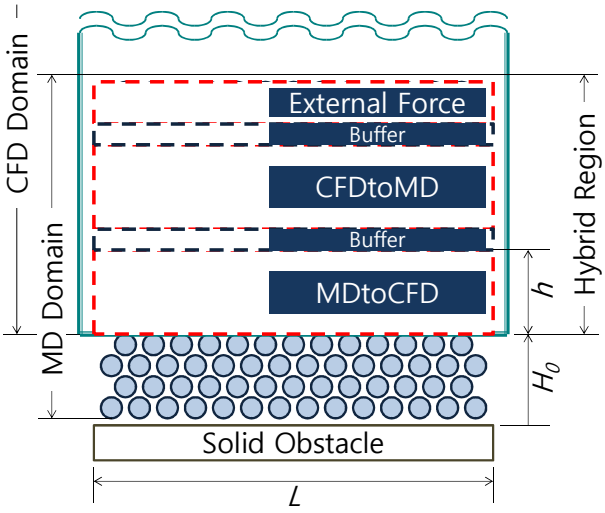

Fig. 1. Schematic diagram of the hybrid domain with detailed view of the overlapping region.

into three layers. In the bottom layer, denoted *MDtoCFD*, sampled averaged molecular properties are directly imposed as the CFD boundary condition. The continuum solution in the *CFDtoMD* layer is imposed on atoms located in the MD domain; that is, the atoms in this region are "guided" to follow the macroscopic flow velocity, by solving a constrained Lagrangian dynamics equation of motion. In the uppermost layer an external force is added to prevent atoms from freely drifting away from the MD region [2].

Four coupling parameters are introduced to define the sampling condition in the particle-to-continuum boundary condition layer (*MDtoCFD*). These parameters are: i) h, the thickness of the sampling layer, ii) H_0, giving the location of the base of the sampling layer, i.e., its distance from the solid wall. iii) the sampling duration (dt_s), and iv) the sampling interval (dt) defining how often the sampled data is communicated to the continuum domain. In two dimensions, considering the length of the computational domain to be L, all particles located in $L \times h$ domain at distance H_0 above the bottom wall participate in the sampling process. The MD sampling accuracy increases by increasing h (along with L in the case of a periodic system) and dt_s, provided that their magnitudes do not violate corresponding scales of the physical process. The magnitudes of L, h and dt_s directly impact the computational cost of the MD simulation. dt is designed to be longer than dt_s, to provide temporal independence between each MD sample. H_0 is usually chosen large enough, e.g., at least 10σ, where σ represents the atomic or molecular length scale (diameter), such that the sampling layer is located at a reasonable distance above the bottom wall [3] to avoid the direct influence of the solid-liquid interface. The *buffer* zones provide isolation between the constrained regions (*CFDtoMD* and the *External Force*) themselves and the sampling region *MDtoCFD*. The choices of the *buffer*, *CFDtoMD* and *External Force* layer thicknesses are to some extent problem dependent, as is that of

the sampling layer.

2.2 Governing equations and numerical schemes

2.2.1 Computational fluid dynamics

An in-house hydrodynamics solver was used to simulate the incompressible isothermal laminar flow of the chosen test problem. For time-accurate unsteady simulation, a dual time stepping method was adopted and combined with the LU-SGS (lower-upper symmetric Gauss-Seidel) scheme [17] for implicit time integration. The inviscid fluxes are upwind-differenced using Osher's flux-difference splitting scheme [18] and the MUSCL (monotone upstream-centered schemes for conservation laws) approach was used [19] on the inviscid flux calculation for acquiring the higher-order spatial accuracy. Viscous fluxes were calculated using conventional second-order central differencing.

2.2.2 Molecular dynamics

Newton's second law, describing the motion of the atoms in the atomic region, is integrated and the trajectories of all atoms comprising the MD region are resolved in time. In this work the interactions between atoms are described by the Lennard-Jones (LJ) potential [20]. A cut-off distance is introduced to reduce the computational cost and is set to be 2.2σ, where σ is an atomic length characterizing atomic diameter. The equations of motion for atoms are integrated using the velocity Verlet algorithm [20]. The MD simulations were performed using the Large atomic molecular massively parallel simulator (LAMMPS) [14] software package. LAMMPS is a classical molecular dynamics open-source code written in C++ and developed by Sandia National Labs. The constrained Lagrangian dynamics and the coupling interface (to exchange the hybrid boundary condition with a CFD code) have been incorporated in LAMMPS to facilitate the hybrid simulations.

2.2.3 Hybrid formulations and interfaces

Hybrid simulations required the implementation of constrained particle dynamics equations in the LAMMPS MD solver. Our implementation followed the approach of Nie et al. [2]. Specifically, to satisfy the continuity between CFD to MD domains, the motion of the atoms in the *CFDtoMD* layer obey the equations:

$$\ddot{x}_i = \frac{F_i}{m} - \frac{\sum_i^N F_i}{Nm} - \frac{1}{\Delta t_{MD}}\left\{\frac{\sum_i^N \dot{x}_i}{N} - u_J(t+\Delta t_{MD})\right\}. \quad (1)$$

According to this equation of motion the particles located in the *CFDtoMD* layer are accelerated/decelerated by constrained forces such that upon averaging their motion is consistent with the velocity imposed by the adjacent continuum domain.

One can view this hybrid coupling as an interface designed to transfer flow properties from one party, the donor, to another one, the receiver, and vice versa. In our hybrid implementation we developed a file-based hybrid interface that consists of a donor information sender, a monitoring function to scan the arrival of the counterpart dataset, and a hybrid boundary condition receiver. For example, the CFD code first writes the flow solution at the *CFDtoMD* layer, monitors the creation of MD data file and stores the molecular samples at the *MDtoCFD* layer.

3. Hybrid simulations of a moderate-velocity flow field

Two important factors determine the accuracy of a hybrid simulation methodology. These refer to the specific hybrid coupling schemes and to the molecular sampling methodologies. In general, the hybrid schemes/equations determine the accuracy of the solution for a specific atomistic-continuum coupling approach and a number of works have been devoted to design/refine them. These include the alternating Schwarz method [4-6], direct flux exchange [7-9], and constrained Lagrangian dynamics [1-3, 22]. On the other hand, there are very few studies on sampling noise (i.e., statistical errors) of averaged MD properties [5, 9] that have been published, even though ultimately these averaging methodologies determine the accuracy of the CFD solution by means of a continuum hybrid boundary condition. In this section, we discuss how to numerically reduce the sampling noise without decreasing the accuracy of the hybrid solution.

3.1 Statistical error due to thermal fluctuations

In the analysis of the average velocity and deviation from the average velocity in a particle simulation of a fluid Hadjiconstantinou et al. [5] defined the statistical fractional error, E_u, of the sampled velocity, u, as the ratio of its standard deviation, σ_u, to the average fluid velocity, u_{x0}, as:

$$E_u = \frac{\sigma_u}{|u_{x0}|} = \frac{\sqrt{\left\langle (\delta u_x)^2 \right\rangle}\Big/\sqrt{M}}{|u_{x0}|} = \sqrt{\frac{kT_0}{m}} \cdot \frac{1}{\sqrt{MN_0}} \cdot \frac{1}{|u_{x0}|} \quad (2)$$

where k is Boltzmann's constant, T_0 refers to the average temperature, and m is the mass of the atoms. M denotes the number of independent samples considered, and N_0 is the average number of particles in the averaging cell. Each sample is considered independent if a sample satisfies the local equilibrium condition, i.e., the time interval between distinct samples is longer than the autocorrelation time of the process, i.e., the collision time τ_{col} ($= 0.14\rho^{-1}T^{0.5}$). Thus, M is expressed in terms of the coupling parameter as $M = dt_s/\tau_{col}$. N_0 is also rewritten as $\rho \times L \times h$, where ρ is the particle number density (assuming that the thickness of the simulation system is w = 1).

Eq. (2) explains why the sampling noise characterizing the hybrid solution is relatively large in a low-speed flow simulation. Specifically, let us consider the same fluid system with

half the average velocity, i.e., $1/|u_{x0}|$ is doubled. Since the first term ($\sqrt{kT_0/m}$) is fixed by the characteristics of the fluid particle and temperature, the product of the number of samples and particles in the representative sampling volume (MN_0) should be quadrupled to maintain the same statistical error. Since ρ and T are fixed in the incompressible isothermal fluid, $dt_s \times L \times h$ should be quadrupled to satisfy the above criteria. Recalling the conditions for coupling parameters described in Sec. 2.1., dt_s is difficult to increase since it is bound by the characteristic time of the process. The increase of both h and L leads to the increase of the MD simulation domain. Clearly, any simulation that contains a representation of the system at atomic level is prone to increased errors as the velocity of the fluid decreases. Thus, numerical approaches need to be developed for reduction of the statistical sampling errors in both particle and hybrid continuum-particle simulations.

3.2 Numerical approaches to reduce the statistical sampling errors

We propose numerical approaches to further reduce the statistical sampling noise in hybrid CFD-MD simulations. Our approach involves i) solving multiple replicated systems for the final solution (see Sec. 3.2.1), which is a way of virtually increasing L, and ii) numerically increasing sampling window sizes (h or dt_s) through either spatial regression (see Sec. 3.2.2) and/or temporal regression (see Sec. 3.2.3).

3.2.1 Multiple replica sampling

The replica exchanging approach [23] has been widely used in molecular dynamic simulations. Essentially, one solves multiple copies of the system with random initialization and exchanges individual configurations during the runtime. In the hybrid CFD-MD application, we ran K independent replicas with different Maxwell-Boltzmann distribution of fluid atoms and average those individual results to obtain a final solution. This averaged solution shows the same order of sampling noise as a single hybrid solution from a K-times larger domain along its periodic direction. Thus, instead of trying to find the optimal domain size and/or coupling parameters for each problem, we repeat replica simulations until we reduce the fluctuation in the solution below the desired threshold. The clear benefit of this approach is that it, in principle, provides a noise-free solution if K → ∞ for any flow simulation regardless of geometric complexity. On the other hand, this approach does not save much in terms of the computational cost, and it merely splits one large task into multiple smaller ones.

3.2.2 Spatial regression

The linear regression method is applied over multiple spatial samples to obtain the hybrid CFD boundary condition. Multiple statistical cells above and under the *MDtoCFD* layer are located along the non-periodic direction. The individual cell has the same dimension as the *MDtoCFD* layer and the same number of cells is piled over and under the *MDtoCFD* layer so that the CFD boundary zone is located in the middle of the stack. Other hybrid layers are shifted upward accordingly, to preserve the layer configuration.

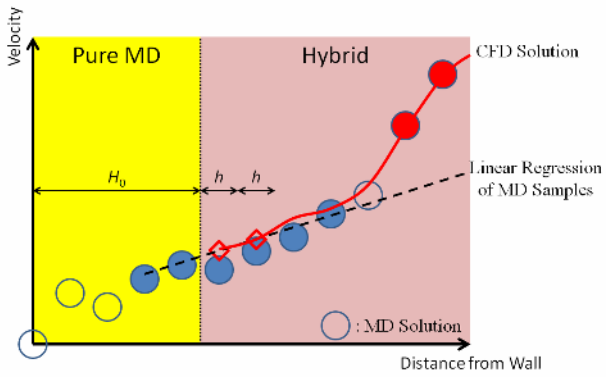

Fig. 2. Linear regression method of spatial samples; Hybrid CFD boundary condition is acquired by the regression curve from multiple samples along the wall-normal direction.

Fig. 2 presents the simple linear regression function (i.e., the ordinary least square estimator) for the current collocated grid formulation. We allocate two additional statistical cells over and under two neighboring CFD ghost cells. Compared to designing two distinct *5h*-height *MDtoCFD* layers, the application of the regression function provides the same level of sampling noise with relatively smaller increase of computational cost.

3.2.3 Temporal regression

The linear regression method is applied over multiple spatial samples to obtain the hybrid CFD boundary condition. We locate multiple statistical cells over and under the *MDtoCFD* layer along the non-periodic direction. Each individual cell has the same size as the *MDtoCFD* layer and the same number of cells is piled over and under the *MDtoCFD* layer so that the CFD boundary zone is located in the middle of the stack. Other hybrid layers are shifted upward accordingly, to preserve the layer configuration.

The first-order linear regression function is applied over previous *MDtoCFD* samples as seen in Fig. 3, for the purpose of virtually increasing the sampling duration dt_s. Considering that J previous samples from t-(J-1)dt to t participate in the regression process, a hybrid CFD boundary condition from t to $t+dt$ is obtained as follows:

$$\begin{aligned} &From\ N\ datasets\ of\ \{x_i, y_i\} = \{t-(J-i)dt, MD_i\} \\ &\quad where\ i = 1,\ldots,J, \\ &CFD(t+\alpha\cdot dt) = a(t+\alpha\cdot dt)+b \qquad (0 \le \alpha \le 1) \\ &\quad where\ a = \frac{\overline{xy}-\overline{x}\,\overline{y}}{\overline{x^2}-\overline{x}^2},\ b = \overline{y}-a\overline{x}, \end{aligned}$$

where MD_i denotes a sampled molecular dynamic solution at i^{th} time step.

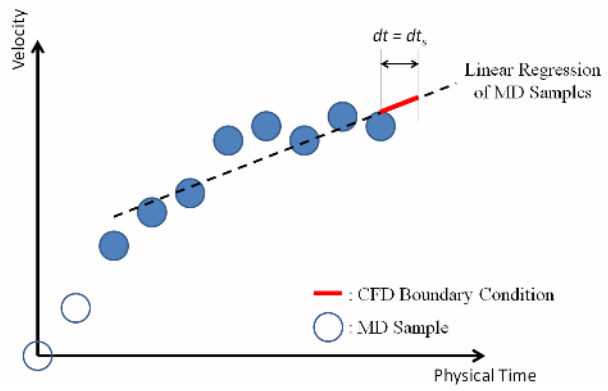

Fig. 3. Linear regression of multiple temporal samples; Hybrid CFD boundary conditions are extrapolated from the linear regression function.

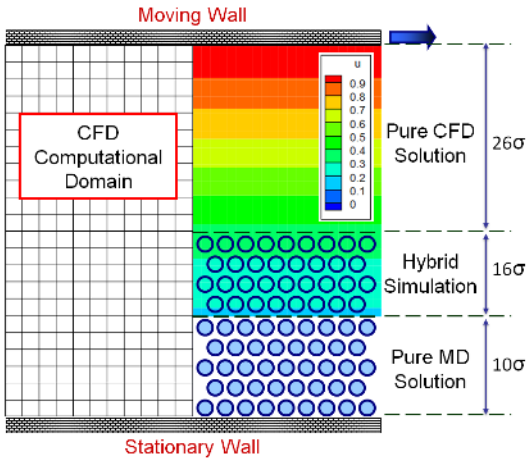

Fig. 4. Computational domain of the Couette flow simulation; The height of the fluid domain is 52σ (≈177Å). The CFD mesh size is 121×27 and the CFD cells at the pure MD region are not updated during the simulation. MD domain size is roughly 204σ along the principal flow direction and around 26σ along the wall-normal direction.

Compared to the spatial regression, the regression of temporal profiles does not increase the computational cost at all. On the other hand, the prediction is performed outside the range of the data so it may provide the wrong solution unless the homogeneity of variance is satisfied.

4. Numerical experiments

4.1 Problem description and validation

The transient Couette flow field has been simulated by a number of investigators for the validation of a hybrid CFD-MD solver. The geometric configuration is a nano-scale channel, which is filled with liquid argon. The characteristic length of liquid argon is $\sigma = 3.405\times10^{-10}$ m and time scale is $\tau = 2.2\times10^{-12}$ sec. The density is $0.81m\sigma^{-3}$, which means that 0.81 atoms are included in the characteristic volume. The wall material consists of "frozen" argon particles whose characteristic properties are the same as liquid argon. The slip ratio between fluid and solid particles is set to 0.6 [2, 3] so that a no-slip condition is macroscopically enforced on the wall during the MD simulation. As presented in Fig. 4, the height of the channel is 52σ. The CFD mesh system is generated over the whole flow field while the pure MD region is treated as a "hole" cell and not updated. The particle lattice is constructed on the bottom half of the fluid domain. Pure MD region is 10σ in height from the bottom wall and the hybrid region is placed on the top of the pure MD region. It consists of eight sublayers each 2σ thick in the vertical direction. Two *MDtoCFD* layers right ahead of the pure MD region and two *CFDtoMD* layers from 18σ to 22σ are separated by two-layer buffer zones in between. A buffer is added above the *CFDtoMD* layer and the external force layer is placed at the top of the hybrid region, above 24σ.

The flow is initially set at rest and the atomistic layer is allowed to reach equilibrium. Then the top wall starts moving by a constant, and relatively high, velocity (1.0 σ/τ) to form the transient Couette flow profile. Fig. 5 presents the hybrid solution velocity profile for the impulsively-started Couette flow. The hybrid solution globally agrees very well with the analytic solution [24]. This proves that the current hybrid framework works.

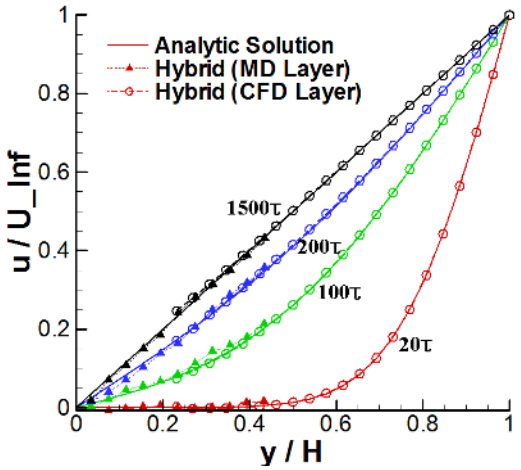

Fig. 5. Impulsively-started Couette flow; the CFD solution is the instantaneous profile at each specified time, and the MD solution is averaged over 2σ in height and 10τ in time.

4.2 Moderate-velocity flow simulation

The impulsively-started Couette flow velocity profile solution for an upper wall velocity of $0.25\sigma/\tau$ is presented in Fig. 6. All other conditions such as the fluid material, domain sizes and coupling parameters are identical to the above validation problem. As we argued in Sec. 3.1, a single solution suffers from strong sampling noise due to the reduced mean velocity. This necessitates the implementation of numerical ideas to suppress the sampling noise for solving for moderate-velocity flow flows. We apply numerical ideas in Sec. 3.2 to the cur-

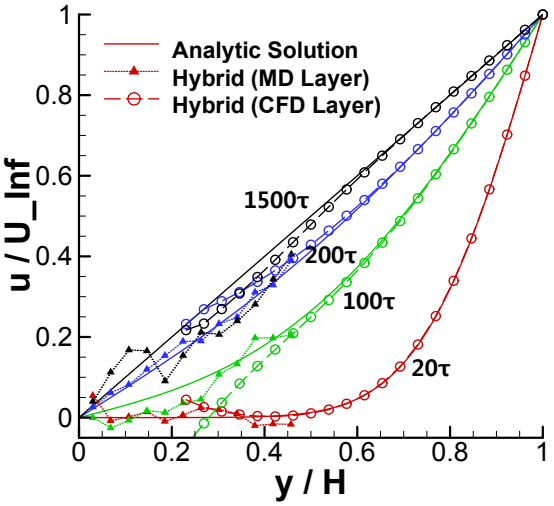

Fig. 6. Couette flow velocity profile for upper plate velocity of 0.25 σ/τ; the solution is very noisy because of the inadequate for low velocities statistical sampling. Red lines denote the solution at 20 τ. Green, blue and black lines are solutions at 100, 200 and 1500 τ, respectively.

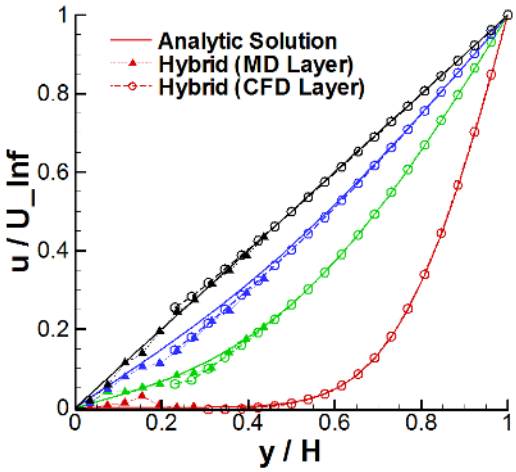

Fig. 8. Impulsively-started Couette flow velocity profiles resulting from the enlarged 16 L system length for a 0.25 σ/τ upper-plate velocity; The sampling noise is significantly suppressed and the solution overall follows the analytic solution, albeit not as well as the averaged result of 16 system replicas (compare with Fig. 7).

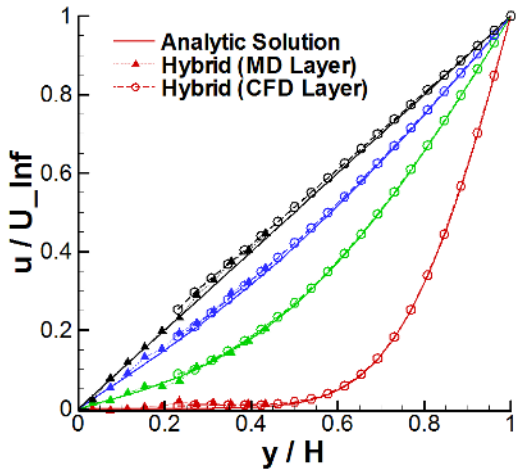

Fig. 7. 16 replica Impulsively-started Couette flow velocity profiles resulting from the averaged 16 system replicas for a 0.25 σ/τ upper-plate velocity; The sampling noise is significantly suppressed and the solution overall follows the analytic solution very well.

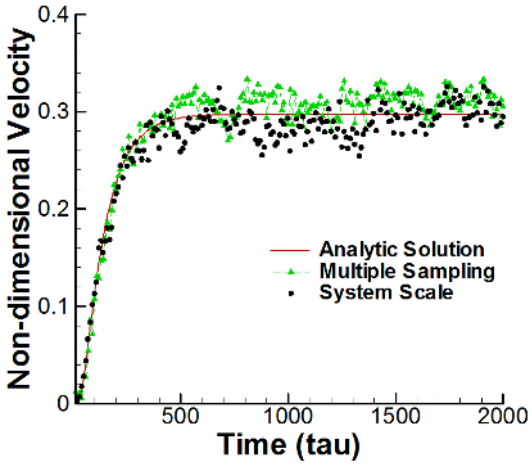

Fig. 9. Variation of the velocity in the middle of the overlap region; Solutions by multiple replica sampling and a single simulation under the increased domain present similar fluctuation strength, which is around 5% of the analytic velocity magnitude.

rent application and discuss the accuracy and effectiveness of each approach.

4.2.1 Multiple replica sampling

According to Sec. 3.1, solving the low velocity flow field of u/m requires increasing the sampling scale by m^2 times to maintain the same order of accuracy as the single solution of the referential velocity of u. So we perform 16 replica simulations each with the same initial system size and average these solutions to numerically increase the spatial sampling scale by 16 times. We compare this result (Fig. 7) with a single solution from 16-times larger MD domain along the principal flow direction (Fig. 8) to verify the accuracy of the proposed approach.

The accuracy of the two solutions is quantitatively compared by plotting the history of the velocity profile in the middle of the overlapping region ($y = 0.3H$). As shown in Fig. 9 hybrid solutions at steady state are on average within 4 % of the analytic solution. In detail, averaging multiple solutions of the smaller system predicts a little faster velocity than the analytic solution, while the solution of the large-scale system fluctuates a bit more. Considering the similar solution accuracy of the two numerical experiments and the computational convenience of running multiple smaller jobs than a large-scale simulation, the multiple replica sampling approach can replace the increase of system size for solving flows of mod-

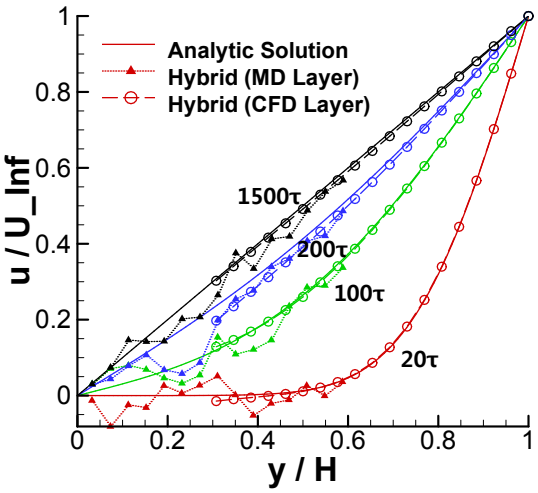

Fig. 10. Spatial sampling of ten wall-normal (vertical) layers; Very noisy MD samples averaged from individual layers are used to obtain the hybrid CFD boundary condition by linear regression. Thus the CFD solution becomes very close to the analytic solution.

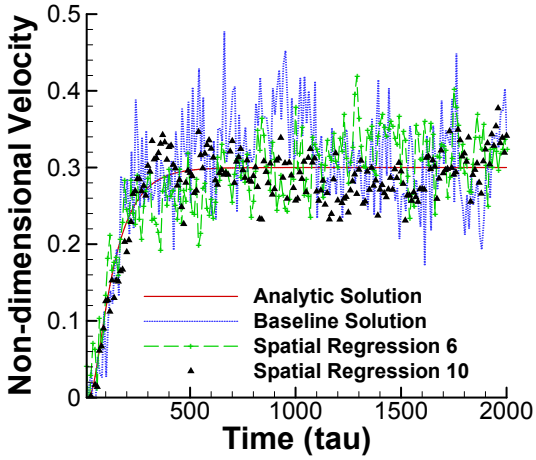

Fig. 11. Noise suppression by spatial regression; linear regression from multiple vertical layers provide less noisy solution than the individual simulation.

erate velocities.

4.2.2 Spatial regression

An impulsively-started Couette flow velocity profile obtained after implementing the spatial regression scheme is presented in Fig. 10. In this simulation, the linear regression function from 10 vertically-consecutive layers was acquired. Each layer was 2 σ in height, spanning overall from 2 σ to 22 σ along the wall-normal direction, so that the hybrid CFD boundary region is placed at the same level as in the previous simulations. Since four additional layers were stacked on the top of *MDtoCFD* region, other hybrid layers (*CFDtoMD*, *External Force* and *Buffer*) were also shifted up accordingly. Each individual MD profile from each layer suffers from the excessive statistical noise, while the CFD solution comes very close to the analytic solution since the regressed MD solution is imposed as the hybrid boundary condition.

The effect of vertically increasing the sampling layer is clearly demonstrated by Fig. 11. From the history of the velocity profile in the middle of the overlap region ($y = 0.3h$), the steady-state solution becomes less noisy with more samples participating in the regression process. The statistical error (Eq. (2)) of each solution after the flow fully converged from the macroscopic point of view was computed as 0.1836 in the case of the baseline simulation without regression. The error is reduced to 0.1121 when six vertical layers participate in the regression and to 0.1040 in the case of ten-layer regression. Regression of ten layers does not show much improvement compared to six-layer regression, because the bottom layer is located closer to the solid wall where stronger molecular interaction takes place. It implies that the spatial regression is more or less limited in suppressing the sampling noise and should be applied in conjunction with other noise suppression techniques such as the multiple replica sampling.

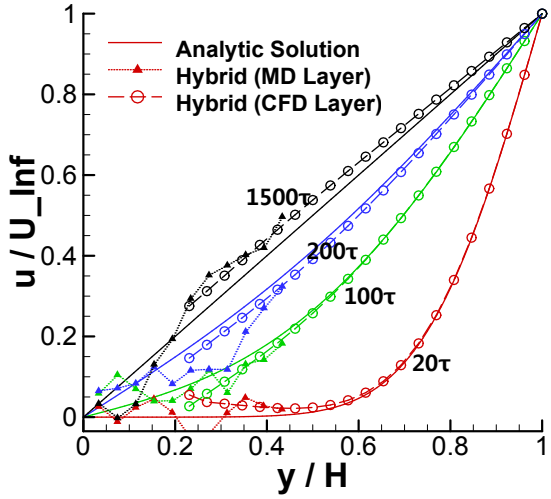

Fig. 12. Impulsively-started Couette flow velocity profiles obtained with implementation of temporal regression scheme using ten previous-to-current temporal solutions.

4.2.3 Temporal regression

An impulsively-started Couette flow velocity profile obtained after implementing the temporal regression scheme is presented in Fig. 12. The history of the velocity profile at the middle of hybrid region is presented in Fig. 13. Compared to the default implementation in which two sampled MD properties at t and t-dt are extrapolated to impose the hybrid CFD boundary condition from t to t+dt, the current simulation uses linear regression in time of ten previous-to-current sampled solutions to update the CFD boundary condition until the next data exchange.

A superficial comparison between Figs. 10 and 12 might

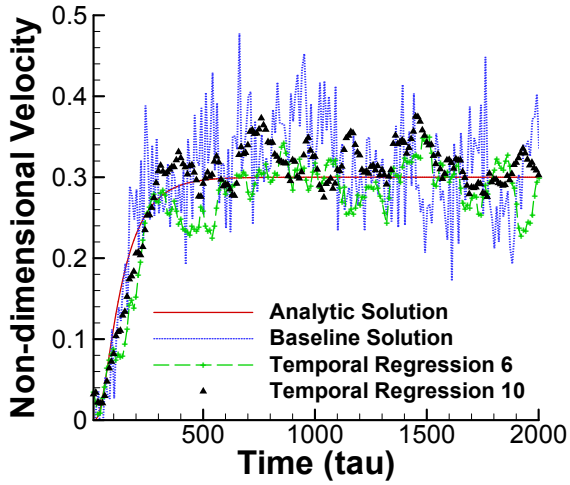

Fig. 13. Noise suppression by the linear regression of multiple temporal sample profiles; compared to spatial regression, the solution becomes less fluctuating.

lead to the erroneous conclusion that the spatial regression is more effective in suppressing the sampling noise. The comparison of the statistical error in the middle of hybrid layer proves the opposite. As can be expected from Fig. 13, the velocity history by the imposition of temporal sampling shows less of a noisy pattern compared to the case of spatial regression. Quantitatively, the magnitude of the statistical error is computed as 0.0945 with six temporal samples and 0.0734 with ten temporal samples. It expresses that the increase of the temporal window is more effective in reducing sampling noise than increasing the spatial scale along the wall-normal direction. Also, further suppression of statistical noise by increasing temporal samples from six to ten is quite reasonable. According to the mathematical expression of sampling noise in Sec. 3.1, the magnitude of the noise is proportional to the square root of temporal scale: The reduction ratio ($=0.0734/0.0945$) from the temporal regression is almost identical to the square root of number of temporal samples ($=\sqrt{6/10}$). The conclusion is that this temporal regression can be effectively applied when simulating the steady-state flow where the unfavorable time-lagging phenomenon during flow evolution is less important.

5. Conclusions

Numerical approaches for accurate hybrid CFD-MD simulation of flows at moderate velocity magnitude have been investigated for the classical test problem of impulsively-started Couette flow. Based on reliable CFD and MD codes employing constrained Lagrangian dynamics for imposing the continuum solution on the atomistic domain, a number of numerical approaches have been designed to determine the CFD boundary condition from the local MD solutions in hybrid simulations. The approaches introduced aim to reduce sampling noise of an individual atomistic solution at lower-speed flows, which are more susceptible to sampling errors. Multiple replica sampling results in hybrid solutions with reduced sampling noise effects, and can be applied to any flow problem, especially non-periodic problems that will suffer from the excessive statistical error due to the limited spatial and temporal sampling scales. Spatial and temporal regressions contribute in getting more accurate solutions from a single simulation run. These approaches were demonstrated on impulsively-started transient Couette flow simulations with maximum average velocities of O (10 m/s), which has not been attempted much because of the excessive computational requirement for acquiring noise-free solutions. The multiple replica sampling approach is verified to provide the same order of accuracy (slightly better in fact) as a single large-scale simulation with the same computational cost. Spatial/temporal regression of multiple layers/time-instants provides some suppression of sampling noise compared to the regression-free, single-run baseline. We expect that these regression methods will contribute to reducing the number of replica runs for acquiring a solution of comparable accuracy at a lower computational cost.

Acknowledgment

This work has been accomplished under the Cybertools (http://cybertools.loni.org) project and was primarily funded by NSF/LEQSF (2007-10)-CyberRII-01. This work has also been made possible thanks to computer resources provided by TeraGrid TRAC TG-MCB090174 and LONI resources.

Nomenclature

dt_s	: Sampling duration
dt	: Sampling interval
h	: Sampling layer size (in height)
H_0	: Position of the sampling layer in vertical direction
L, H	: Length and height of the fluid domain
σ	: Non-dimensional molecular length unit
τ	: Non-dimensional molecular time unit
m_i	: Non-dimensional molecular mass for i^{th} particle
F_i	: Non-dimensional molecular force for i^{th} particle

References

[1] S. T. O'Connell and P. A. Thompson, Molecular dynamics continuum hybrid computations: a tool for studying complex fluid flows, *Phys. Rev. E*, 52 (1995) R5792-R5795.

[2] X. B. Nie, S. Y. Chen, W. N. E and M. O. Robbins, A continuum and molecular dynamics hybrid method for micro- and nano-fluid flow, *J. Fluid Mech.*, 500 (2004) 55-64.

[3] T. H. Yen, C. Y. Soong and P. Y. Tzeng, Hybrid molecular dynamics-continuum simulation for nano/mesoscale channel flow, *Microfluid Nanofluidics*, 3 (2007) 665-675.

[4] N. G. Hadjiconstantinou and A. T. Patera, Heterogeneous

atomistic-continuum representations for dense fluid systems, *Int. J. Mod Phys C*, 8 (1997) 967-976.
[5] N. G. Hadjiconstantinou, A. L. Garcia, M. Z. Bazant and G. He, Statistical error in particle simulations of hydrodynamic phenomena, *J. Comput. Phys.*, 187 (2003) 274-297.
[6] T. Werder, J. H. Walther and P. Koumoutsakos, Hybrid atomistic-continuum method for the simulation of dense fluid flows, *J. Comput. Phys.*, 205 (2005) 373-390.
[7] E. G. Flekkoy, G. Wagner and J. Feder, Hybrid model for combined particle and continuum dynamics, *Europhys. Lett.*, 52 (2000) 271-276.
[8] R. Delgado-Buscalioni and P. V. Coveney, Usher: An algorithm for particle insertion in dense fluids, *J. Chem. Phys.*, 119 (2) (2003) 978-987.
[9] R. Delgado-Buscalioni and P. V. Coveney, Hybrid molecular-continuum fluid dynamics, *Philos. Trans. R. Soc. London, Ser. A*, 362 (2004) 1639-1654.
[10] The open source CFD toolbox (OpenFOAM), *http://www.openfoam.com/*.
[11] Nek5000, *http://nek5000.mcs.anl.gov/index.php/Main_Page*.
[12] Code_Saturne, *http://code-saturne.org/cms/*.
[13] Edge, *http://www.foi.se/edge*.
[14] LAMMPS, *http://lammps.sandia.gov*.
[15] GROMACS, *http://www.gromacs.org/*.
[16] NAMD, *http://www.ks.uiuc.edu/Research/namd/*.
[17] S. Yoon and A. Jameson, Lower-upper symmetric-gauss-seidel method for the Euler and Navier-Stokes equations, *AIAA J.*, 26 (1988) 1025-1026.
[18] M. M. Rai and S. R. Chakaravarthy, An implicit form of the Osher upwind scheme, *AIAA J.*, 24 (1986) 735-743.
[19] B. V. Leer, Towards the ultimate conservative difference scheme. V. A second order sequel to Godunov's methods, *J. Comput. Phys.*, 32 (1979) 101-136.
[20] M. Allen and D. Tildesley, *Computer simulation of liquids*, Oxford Science Publications (1987).
[21] K. Travis and K. Gubbins, Poiseuille flow of Lennard-Jones fluids in narrow slit pores, *J. Chem. Phys.*, 112 (2000) 1984-1994.
[22] S.-H. Ko, N. Kim, D. E. Nikitopoulos, D. Moldovan and S. Jha, Parametric study of a multiscale fluidic system using a hybrid CFD-MD approach, *Proc. of the 5th European Conference on Computational Fluid Dynamics (ECCOMAS CFD 2010)*, Lisbon, Portugal (2010).
[23] Y. Sugita and Y. Okamoto, Replica-exchange molecular dynamics method for protein folding, *Chem. Phys. Lett.*, 314 (1999) 141-151.
[24] A. A.Mendiburu, L. R. Carroccib and J. A. Carvalho, Analytical solution for transient one-dimensional Couette flow considering constant and time-dependent pressure gradients, *Engenharia Térmica (Thermal Engineering)*, 8 (2) (2009) 92-98.

Soon-Heum Ko is a computational scientist at the Swedish National Supercomputing Center in Linkoping, Sweden. He received his Ph.D. in aerospace engineering in 2008 from Seoul National University. Later he served as a post-doctoral fellow at Louisiana State University in USA and joined the Swedish National Supercomputing Center in 2011. His research interests are in the multi-scale flow simulation and high performance computing.

Nayong Kim is on the research staff at the Center for Computation & Technology (CCT) and Louisiana Biomedical Research Network (LBRN) Bioinformatics / Biocomputing Core (BBC) member. He has a Ph.D. in Chemical Engineering and MS in both Computer Science and Chemical Engineering from University of Southern California.

Dorel Moldovan is an Associate Professor in the Department of Mechanical and Industrial Engineering at Louisiana State University. He obtained his Ph.D. in 1999 in Physics from West Virginia University. His recent research focuses on the development of fundamental understanding of various transport and surface and interfacial phenomena in biomolecular systems.

Dimitris E. Nikitopoulos is a Professor in the Department of Mechanical and Industrial Engineering at Louisiana State University. He obtained his Ph.D. in 1987 in Engineering (Fluid Dynamics and Applied Mathematics) from Brown University. His research interests include multi-phase flows, micro-/nano-fluidics, multi-scale modeling using hybrid continuum/atomistic techniques, Bio-MEMS/NEMS, and gas-turbine aerodynamics and heat transfer.

Shantenu Jha is an Assistant Professor at Rutgers University. Before moving to Rutgers, he was the lead for Cyberinfrastructure Research and Development at the CCT at Louisiana State University. His research interests lie at the triple point of Applied Computing, Cyberinfrastructure R&D and Computational Science.